Desalination and Water Treatment
www.deswater.com
1944-3994/1944-3986 © 2013 Desalination Publications. All rights reserved
doi: 10.1080/19443994.2012.699448

51 (2013) 1091–1103
January

Taylor & Francis
Taylor & Francis Group

Assessment of silt density index (SDI) as fouling propensity parameter in reverse osmosis (RO) desalination systems

R.M. Rachman, N. Ghaffour*, F. Wali, G.L. Amy

Water Desalination and Reuse Center, King Abdullah University of Science and Technology (KAUST), Thuwal, Saudi Arabia
Tel. +966 28082180; email: noreddine.ghaffour@kaust.edu.sa

Received 5 March 2012; Accepted 29 May 2012

ABSTRACT

Due to its simplicity, silt density index (SDI) is extensively used in reverse osmosis systems despite its limitations in predicting membrane fouling. Employing a reliable fouling index with good reproducibility and precision is necessary. The aim of this investigation is to assess the reliability of SDI in order to understand the reasons for the low level of precision and accuracy. Different commercial SDI membranes and feedwater quality were used in this study. Results showed the existence of membrane properties' variation within manufacturers, which then causes a lack of accuracy in fouling risk estimation. The nature of particles during SDI filtration provides information that particle concentration and size play a significant role in SDI quantification with substantial representation given by particles with size close to membrane nominal pore size. Moreover, turbidity-assisted SDI measurements along with determination of ultrafiltration permeate and clean water fouling potential, establish the indication of nonfouling-related phenomena involved on SDI measurement such as natural organic matter adsorption and hydrodynamic conditions that alters during filtration. Additionally, it was found that the latter affects the sensitivity of SDI by being represented by some portions of SDI values.

Keywords: Assessment of SDI; RO membrane fouling prediction; Fouling indices; Particulate fouling; SDI membrane characterization

1. Introduction

A fouling evaluation tool is required to determine the feedwater fouling potential and to monitor the efficiency of the pretreatment processes. Precise prediction of the fouling potential by a fouling index is critical to ensure the steady operation of a reverse osmosis (RO) desalination plant. Thus, employing a reliable fouling index, in terms of good reproducibility and precision, to analyze the fouling tendency of pretreatment effluent for RO feed system is a necessity. Silt density index (SDI) is the most widely used fouling potential determination tool for RO feed water. SDI measurement is a convenient, simple, and brief practice to be performed routinely by plant operators even without special training [1]. The demonstration of SDI measurement conducted to evaluate the pretreatment processes of the seawater reverse

*Corresponding author.

Presented at the International Conference on Desalination for the Environment, Clean Water and Energy, European Desalination Society, 23–26 April 2012, Barcelona, Spain

osmosis (SWRO) facility at King Abdullah University of Science and Technology (KAUST) was conducted.

Unfortunately, this simple tool is often found failed in predicting the propensity of the membrane fouling. The reproducibility of SDI results has been found to be deficient in precision simply in regard to system operation and lead to lack of precision in predicting the fouling potential. SDI values for the same water sample can be varied due to the measurement practices by the operator [2]. SDI apparatus/kit confirmed to give some variation in the value of SDI for the same kind of water [2,3]. The SDI membrane also fails to give the precise value of SDI when the measurements are conducted with membrane variation [4]. As mentioned in the standard test method for SDI of water, the SDI varies with the membrane filter manufacturer so that the values obtained with filters from different membrane manufacturers cannot be comparable. Threefold difference of SDI values was reported when comparing various hydrophobicity membrane materials [5]. Other properties of membrane such as pore size distribution (PSD), thickness, roughness of the membrane, and membrane resistance were studied [4] that resulted in significant variation between material, manufacturers even in the different batch of the same manufacture. In relation to precision matter, two different commercial membranes were investigated in this study to describe the precision of SDI measurements in regard to variation of membrane properties.

The SDI measures inaccurately the fouling potential of RO feedwater and corresponds to an over/underestimation. Actual RO plants experience severe fouling phenomena when exploiting low SDI values [6–8]. In addition, low turbidity water and ultrafiltration (UF) pretreated water have been found to have high SDI value, which demonstrates peculiar phenomena behind the measurement. Along with the utilization of SDI as fouling index, doubts have been raised concerning the reliability of SDI in regard to predicting fouling occurrences in RO systems. SDI calculation as shown in Eq. (1), essentially is based on none of the classical filtration mechanism equations [9,10].

$$\mathrm{SDI}_T = \frac{\%P_{30}}{T} = \frac{1}{T}\left[1-\frac{t_1}{t_2}\right] \times 100\% \quad (1)$$

where $\%P_{30}$ indicates the plugging rate of membrane at 30 psi pressure. The time parameter t_1 is determined as the time required to collect the first 500 mL filtrate. After the filtration elapses for T (15 min), the time t_2 needed for collecting final 500 mL of filtrate is measured. Then, the SDI value is calculated and presented in %/min. Rearranging the original Eq. (1) in the following form,

$$\mathrm{SDI}_T = \frac{1-\left(\frac{500}{t_2}:\frac{500}{t_1}\right)}{T}\,100\% \quad (2)$$

clearly shows that the calculation is simply based on a comparison between two flow rates at two specific times, which are at the beginning and at the end of filtration [11]. Combination of fouling mechanisms can be assumed and considered in SDI measurement, namely cake filtration and blocking filtration, which are likely to happen in such a microfiltration (MF) process [12] and not expected in RO filtration. This unmatched filtration mechanism within low- and high-pressure membrane essentially bring SDI as an improper way to predict the fouling of RO and nanofiltration (NF) operation [13]. SDI also fails to relate the quantity of colloidal matter represented in its value which was unsuccessful to relate the turbidity as a measurement of the amount of suspended solids. Mosset et al. [5] mentioned that an increase in turbidity may not directly be represented in SDI values. In case, if the turbidity barely changes, the SDI triples. The relationship between SDI and the actual foulant deposition has been studied by Kremen and Tanner [14] whose research demonstrated the geometric trend between index values with the mass of captured particles. Some improvements to the SDI method allows data normalization and establishes meaningful comparisons by utilizing the $\mathrm{SDI}_{75\%}$, which is the index value that extrapolated at exactly 75% of plugging [5]. In this work, investigation towards the nature of the SDI filtration and particle removal was studied employing the influence of particle concentration and size.

The SDI values are prone to representing the nonfouling phenomena. Ando and Ishihara [15] hypothesizes that SDI is sensitive to a slight change of a filtration hydrodynamic in the form of micro air bubbles. Moreover, the unexpected result was also found by having a certain value of SDI for UF pretreated water. Previous findings contradict the putative SDI value of water that has been passed through the UF membrane (i.e. 0.02 μm pore size), which is ideally as low as 0, because no more particulates are present in the UF membrane [16–20]. Furthermore, peculiar phenomena in SDI values reported from fouling tendency evaluation of UF filtrates. Significant value of SDI was obtained as the result of UF filtrates fouling risk, with the presence of insignificant particulate after intensive removal through UF pore size. This fact leads to the assumption that particulate foulant is not the sole parameter represented by SDI. Natural organic compound and nonfouling factors, such as micro air bubbles, might also be affecting the SDI result [15]. In

this study, nonfouling-related phenomena described by SDI values were observed by testing the SDI for low-potential fouling water and clean water (UF pretreated water, RO permeate, deionized water, and ultrapure water).

2. Material and methods

2.1. Fouling indices determination

The SDI testing unit used in this work is Aike Portable SDI Tester provided by Horizon Environmental Technology Co., LTD (Fig. 1). The laboratory setup measured the rate of plugging of a membrane filter with nominal pore size of 0.45 μm at 30 psi constant pressure filtration for certain period of time. The measurements were conducted at laboratory condition. Clean water flushing was conducted after every measurements of SDI. The used membrane was carefully collected for imaging characterization using Scanning Electron Microscopy (SEM).

Fifteen minutes filtration time (T) was used as a default operation procedure. Shorter period of filtration was taken for particular samples, which exert high fouling potential. SDI values were calculated using Eq. (1).

2.2. SDI membranes

The membranes used in this work are white disk hydrophilic MF type with nominal pore size of 0.45 μm. The membranes disk diameter and surface area were 47 mm and 13.8 cm^2, respectively. Two commercial membranes identified as MA and MB based on different material, cellulose acetate and mixed cellulose ester, respectively, were used in this investigation. Both membranes were specifically used to demonstrate the membrane properties effect on SDI.

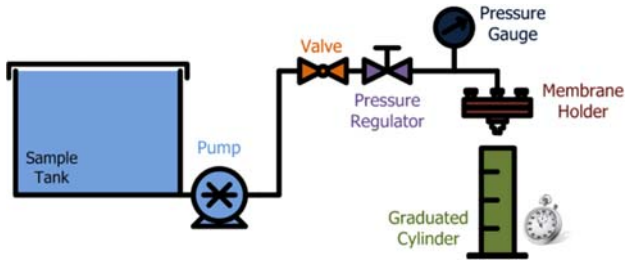

Fig. 1. Laboratory setup for SDI determination.

2.3. Membrane physical characterization

2.3.1. Pore size distribution

Mercury porosimeter technique (Pore Master from Quantachrome) was used to give the PSD and quantify mean pore size. The pore size of the membrane was determined based on the additional energy required to intrude the nonwetting liquid (mercury) through the membrane pore against the surface tension of the liquid.

2.3.2. Membrane hydrophobicity

Measuring the contact angle concluded the hydrophobicity of the membrane. Contact angle is the angle at which a liquid interface meets a surface, and the value depends on the hydrophobicity character of the surface. Higher value of contact angle represents more hydrophobic nature of the membrane and vice versa. The instrument (CAM 200 from KSV Instruments) captures the images of liquid membrane interfaces, which then calculate the contact angle based on the particular shape shown by the liquid. The values of contact angle obtained were used to compare the two membrane samples.

2.3.3. Membrane surface charge

Membrane surface charges were measured using an electrokinectic analyzer (SurPASS from Anton Paar). The measurement of zeta potential was conducted using a 10 mM NaCl solution at different pH values that being adjusted accordingly using 0.1 M of NaOH and 0.1 M of HCl. The measurements' result is the zeta potential of the membrane, calculated using Helmholtz–Smoluchowski equation, as a function of pH.

2.3.4. Clean membrane resistance

Membrane resistance was determined by performing a clean water flux experiment to the membrane samples. Clean water flux was tested by filtration of ultrapure water through a membrane sample under constant pressure. Membrane resistance (R_M) was then calculated using Darcy's Law.

$$J = \frac{\Delta P}{\mu R_M} \tag{3}$$

where ΔP is the applied pressure, J is the flux, and μ is the water viscosity.

2.3.5. Imaging and deposit analysis of the membrane

SEM image analysis was conducted to obtain micrographs of SDI membranes subsequent to water sample filtration. The resulted micrograph of the membrane surface was then analyzed visually and chemically. Visual analysis determined the membrane thickness, pore shape, and qualitative membrane porosity of clean membranes. Meanwhile, for the used membranes, qualitative analysis of foulant existence was conducted. In addition, chemical analysis was conducted to the foulant deposited on the membrane using Energy-dispersive X-ray Spectroscopy (EDX) to determine the specific element of the foulant. This EDX analysis covered certain limited observation area or point of interest over the membrane surface.

2.4. Water samples

In order to demonstrate the application of SDI in predicting fouling potential, three sampling points were considered at KAUST–SWRO. As shown in Fig. 2, these points include spruce filter inlet, spruce filter effluent, and RO feed water (after the cartridge filter). Further in this paper, these points are referred as P1, P2, and P3, respectively. The P3 water was also used to investigate the particle removal during SDI test. The study of the influence of membrane properties utilized one specific kind of water. Clean water such as deionized water, UF pretreated water, RO permeate, and ultrapure water were use to investigate the nonfouling phenomena represented in SDI values. The influence of particle size and concentration towards SDI quantification utilized model water. The samples were made from ultrapure water added with well-defined amount of polystyrene microparticles, monodisperse particles, with specific size. The particle sizes used in this study are 0.1, 0.5, 1 μm, and mixture of aforementioned sizes with equal portion. The variations of particle concentration are 0.5, 1, and 2 ppm. The parameters categorizing water quality involved in this work were particle content, temperature, organic compound analysis, and pH. The particle content of the water samples was determined by turbidity and particle analyzer techniques.

3. Results and discussion

3.1. SDI measurements for KAUST-SWRO facility

We have used SDI measurement to determine the performance of pretreatment process in KAUST–SWRO facility as case study. Both, *in-situ* and lab measurements were compared to understand the reproducibility of SDI determination. The plant utilizes the conventional pretreatment system using spruce media filter as the main treatment for the RO feedwater as shown in Fig. 2. Antiscalant and sodium metabisulfate are injected before and after the cartridge filter, respectively. SDI_5 was performed to analyze P1 as the recommended choice rather than SDI_{15}, because typically filtration of raw seawater through the SDI membrane clogs the membrane before 15 min. P2 and P3 were analyzed normally by performing SDI_{15}. All measurements of SDI were performed in the laboratory (*ex-situ*). The resulted values of SDI are 16.04, 3.55, and 3.01 for P1, P2, and P3, respectively (Fig. 3). The fouling potential, in terms of SDI, is reduced significantly by the spruce media filter, which removed the majority of particulate foulants as depicted by the graph. Ultimate barrier, provided by cartridge filter, removed minor fraction of foulant and reached SDI value of 3.01, which is generally recommended by RO membrane manufacturers [21–25].

These values confirmed the role of the spruce media filter as the main pretreatment process of the SWRO plant. The cartridge filter is dedicated as the ultimate barrier to protect RO membranes when the spruce filter fails to perform the required work. Typically, cartridge filters are used in all RO plants including when UF membranes are used in pretreatment. Spruce multilayer filter is an improved mechanism of regular media filter to remove the solid

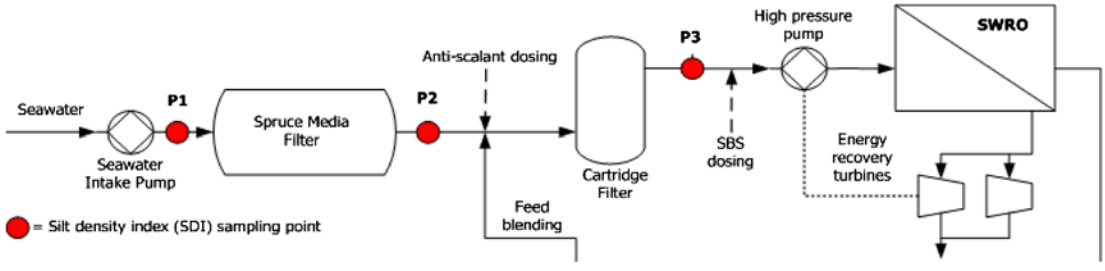

Fig. 2. Simplified pretreatment process flow diagram of KAUST–SWRO plant with three designated sampling points (P1, P2, and P3) for SDI measurement.

matter (colloidal and suspended) with two methods of removal, mechanical retention, and surface adsorption. These dual methods are allowing excellent removal by extract and retain over 99.954% of particle counts down to 0.2 μm without addition of polyelectrolyte or coagulant aid based on an independent product test. The filter bed consists of four layers of inert natural media that have an increasing density and a decreasing particle size. The specific shape factor of the media contributes to simpler backwash fluidization process, with typical backwash water consumption of only 0.1–1% of the forward feed without air scouring required and no use of chemicals.

To understand the physical properties of the SDI membranes, we have taken SEM images of the membrane surface subsequent to the test for points P1 and P3 as shown in Fig. 4. More deposit was found on the membrane after analyzing P1 than on the membrane after analyzing P3. The membrane surface and fouled area can be differentiated easily for the latter membrane describing low foulant content in the water.

Silica is one of the best representations of particulate fouling that designated as the element of interest. To investigate the foulant composition on membrane surface, EDX analysis was conducted. Based on partial spectra of EDX result, shown in Fig. 5, silicon fraction was found at the reduced level on membrane P3 compared to deposit on membrane P1. This silicon element analysis result corresponds mainly to colloidal silica which is effectively removed by spruce filter.

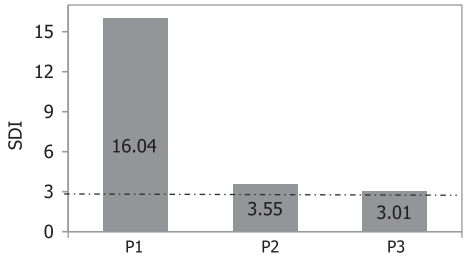

Fig. 3. SDI values along pretreatment process line at KAUST–SWRO plant.

Besides the conclusion that spruce media filter provides proper pretreatment of seawater prior to RO, there is another point that should be noted. During this experiment period, SDI results of P2 that were performed in-situ by the operator was also taken down. In-situ analysis resulted in SDI value below two at most of the time, compared to the laboratory analysis, ended up with 3.55. Given the fact that different kit of SDI apparatus was used in the plant, it seems that the lack of reproducibility and accuracy due to the different measurement system were present.

To investigate this inconsistency in SDI measurements, we have considered an experiment using the same SDI laboratory kit for two commercially available membranes (MA and MB). A specific kind of water was used as sample to determine its SDI with different membranes. Repetitive SDI measurements were performed to investigate the precision of the results. The attention then focuses on the results in terms of measurement reproducibility for each membrane type used and measurement accuracy between the two membrane types. The SDI result is shown in Fig. 6. Interestingly, we have obtained different values for the same source of water with high number of standard deviation. Evidence of the imprecision results of SDI was shown by the standard deviation of measurements within the same type of membrane. SDI of water sample obtained using MA ranging from 3.96 to 4.80, which implied 8.8% in standard deviation. In the same manner, 8.22% was the standard

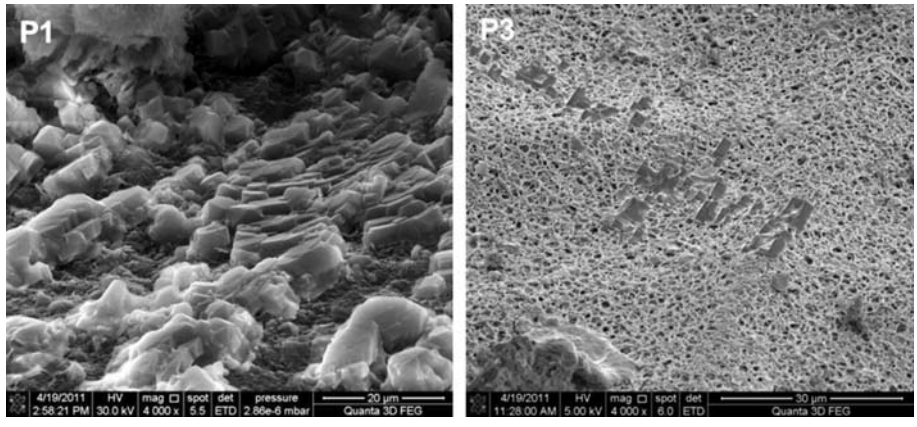

Fig. 4. SEM micrographs of membranes after measuring SDI of P1 and P3.

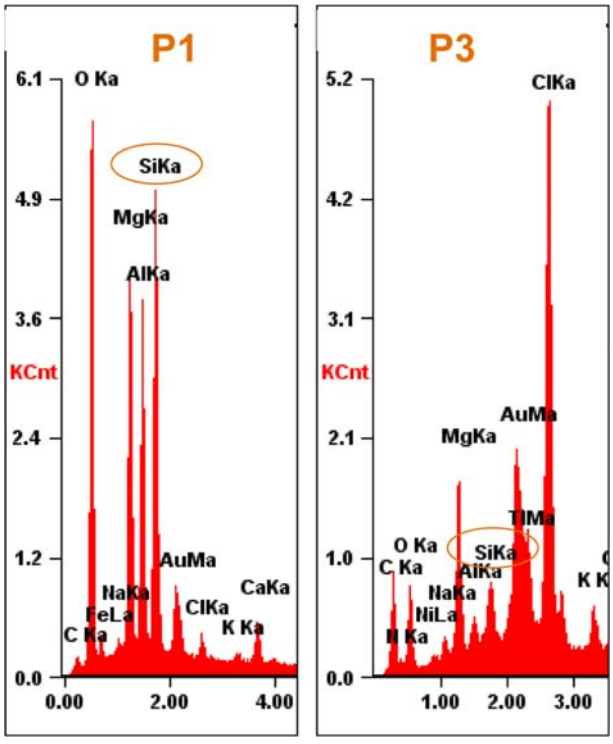

Fig. 5. EDX spectra showing Si as representation of particulate foulant.

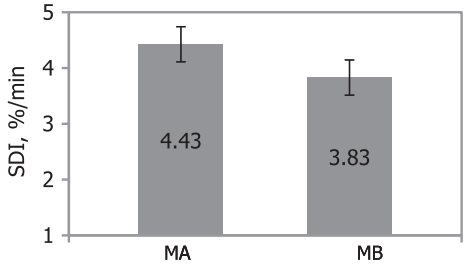

Fig. 6. SDI values of tap water using different commercial SDI membranes MA and MB.

deviation found by having 3.41–4.24 as SDI values when MB was used. This observation illustrates that fouling tendency determination with SDI has the problem with precision and reproducibility. The failure of obtaining converge results towards single value within measuring the same water samples might be caused by variability in measurement techniques and dissimilarity of properties of SDI membrane used in all cases.

Fig. 7 shows the fouled SDI membranes after filtration. Existence of particulate foulant, represented by the SDI, fouled the membranes, mainly by cake build-up on the top of membrane surface as shown by SEM micrograph of fouled membranes surface in Fig. 7. We have assumed that the yellow color of the foulant trapped on the membrane surface indicatesthe presence of large amount of iron in used water sample. EDX analysis of the area shown by micrograph presented in Fig. 8 indicates the agreement of iron (Fe) as main foulant that most probably came from rusted metal fittings along the distribution line. Silicon (Si) element is also found as one of the foulant from elemental analysis, which is greatly related to particulate fouling anticipated by measuring SDI in regard to silica. The existence of silica is naturally complex by having different forms, which are reactive silica and polymerized silica [8]. Reactive silica present in water refers to single constituent silica (SiO_2), which is in equilibrium with bisilicate ($HSiO_3^-$), a very weak acid. Whereas, the polymerized silica consists of long chain of individual silica constituent that is often referred to as colloidal silica. The latter type of silica is the main concern in regard to colloidal fouling, since the removal is typically done by size exclusion filtration. In contrast, reactive silica is in the form of ionic equilibrium, which typically employs ion exchanger to pursue its removal. Thus, Si element that was cap-

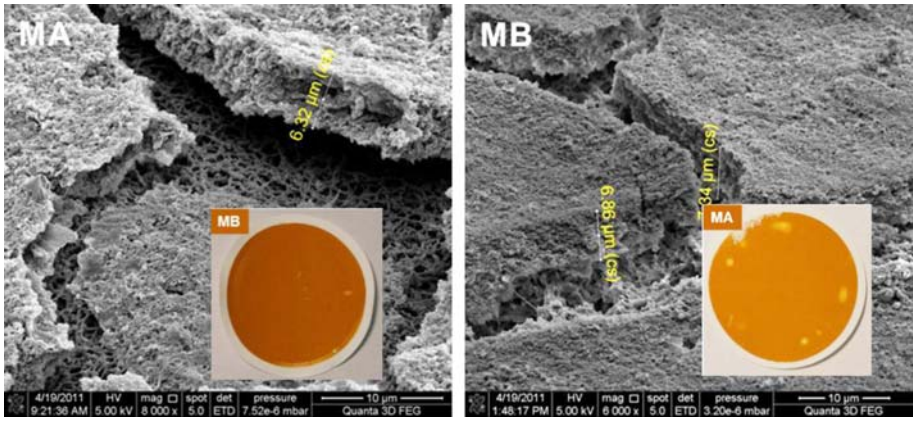

Fig. 7. SEM micrograph of fouled membranes after SDI filtration.

tured in the EDX result is mainly representation of colloidal silica.

3.2. Physical characterization of the SDI membranes used in this study

To understand the difference between both (MA and MB) membranes results, we have investigated their physical properties like their PSD, mean pore size, surface porosity, membrane thickness, membrane resistance, membrane hydrophobicity, and membrane zeta potential. The effect of these properties of membrane associated to the resulted SDI in the previous section will be discussed. Pore sizes of the membranes were characterized by mercury porosimeter to obtain the PSD curve and mean pore size. PSD curve of the two membranes variation is presented in Fig. 9. Broad PSD curve was found for both membranes, suggesting variation in pore size available for filtration. The mean pore size of MA is higher than MB with each value of 481 and 563 nm, respectively. Considering the nominal pore size of the membrane is 450 nm or 0.45 μm as presented in membrane specification, which confirmed the variation between the mean pore size and its nominal value. This diversity of pore size in regard to particulate foulant exclusion in such filtration, affect the rejection absoluteness, which supposedly limited the specified pore size.

Surface porosity was qualitatively determined through surface imaging. SEM micrographs of both membranes are shown in Fig. 10. Pores of MA were found more structurally defined than MB. It is also clear that surface porosity of MB is higher than MA by having more void (empty space) fractions along polymeric structural on the surface of the membrane. SEM technique also utilized to obtain membrane cross-section images, which determine the thickness of corresponding membranes. Micrographs of the cross-sectional areas of both SDI membranes are shown in Fig. 11. Membrane thicknesses of the two SDI membranes are 55.61 and 193.32 μm for MA and MB, respectively. Structural observation to the membranes, both MA and MB, are symmetric with spongy structure. Specifically, for MA, additional fiber-like material incorporated with polymeric structure of the membrane, known as reinforcing material, is observed. The reinforced membrane received an additional support to the structure and typically manufactured with lesser thickness than full asymmetric membrane to deliver comparable strength [26].

In order to relate aforementioned membrane properties to SDI values resulted in utilizing two different kinds of membranes, a lump-sum parameter should be introduced which incorporates pore size, surface porosity, and membrane thickness. The parameter is membrane resistance (R_M), which is simply measured by passing ultrapure water through the membrane and the pressure difference, flux and water viscosity data were noted. Darcy's law was then used to calculate the membrane resistance (Eq. (3)). Theoretically, lower membrane resistance is obtained with smaller membrane thickness, higher porosity, and bigger pore size. Calculated membrane resistances for MA and

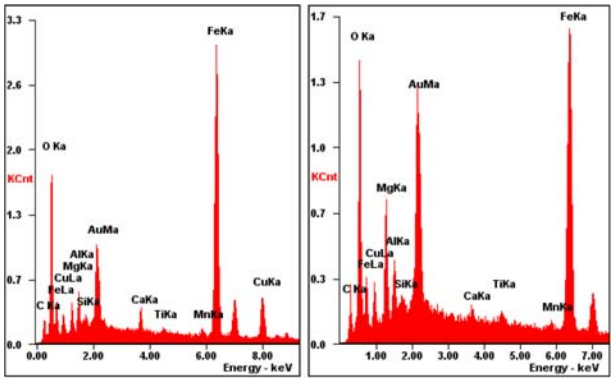

Fig. 8. EDX spectra showing Fe as representation of particulate foulant.

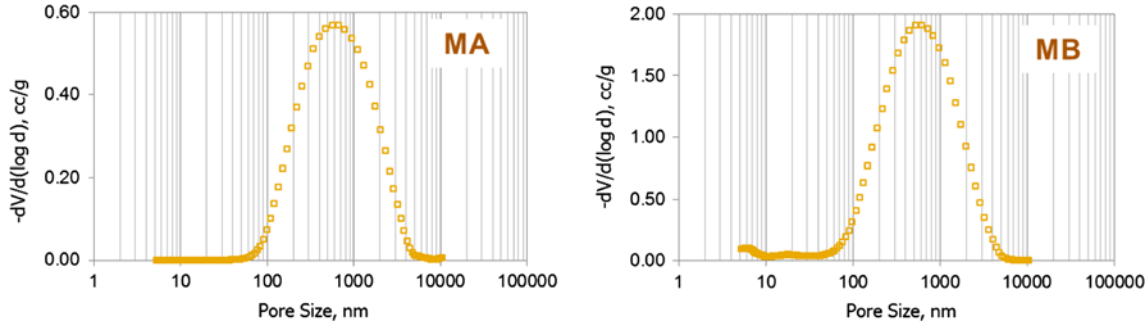

Fig. 9. PSD for both SDI membranes, MA and MB.

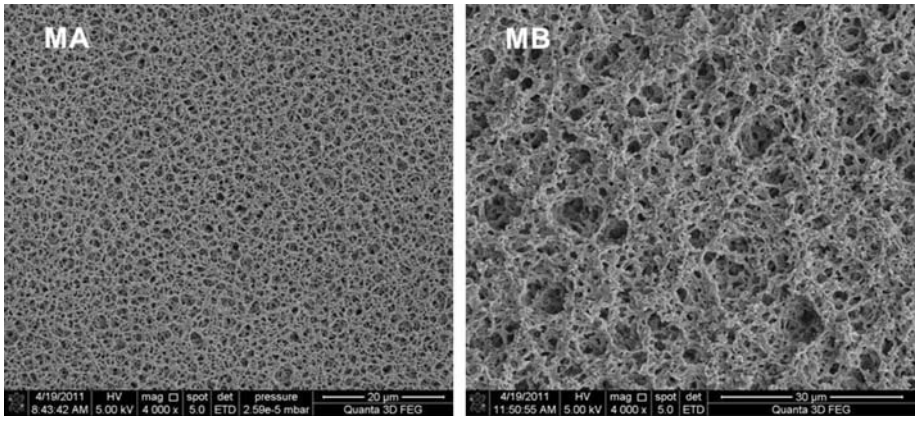

Fig. 10. SEM micrographs of SDI membranes surface for both SDI membranes, MA and MB.

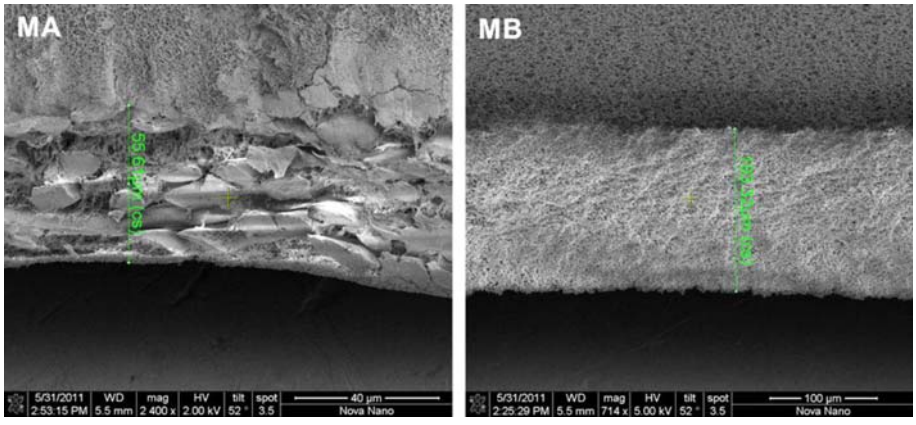

Fig. 11. SEM cross-sectional micrographs for both SDI membranes, MA and MB.

MB membranes are 1.865×10^{10} and $2.06 \times 10^{10}\,m^{-1}$, respectively. Higher membrane resistance of MB over MA agrees with the finding that MB is thicker than MA. However, the trend of mean pore size and surface porosity does not support the tendency of membrane resistance. This can be explained by assuming the significant difference in membrane thickness, which is more influential in determining the membrane resistance than a slight different in mean pore size and qualitative comparison of surface porosity. Lower membrane resistance allows higher flow rate that passes through the membrane, which corresponds, to more foulant to be deposited on the membrane surface. In other words, lower membrane resistance is in accordance to higher fouling capacity/load. Moreover, since SDI measured time as a fixed variable and accumulated volume within the time is relying on the flow rate, fouling capacity of the membrane will elevate with the increasing flow rate. Therefore, SDI measure appears higher. This consideration is being fulfilled by the fact that the result of SDI for MA, which has lower membrane resistance thus enable higher flow rate to pass through, is higher than MB which corresponds to higher resistance and lower flow rate.

Other membrane properties considered to be affecting the SDI measurement is membrane surface charge and hydrophobicity. The surface charge of the SDI membranes describes by zeta potential as a function of pH is shown in Fig. 12. The zeta potential was measured in the 10 mM of NaCl electrolyte solution to include representation of salinity in the water sample. In general, zeta potential is approaching more negative values as pH increases. Surface charge of MA is more negative compared to MB in all values of pH.

The results of the SDI membrane hydrophobicity, represented by the contact angle, are shown in Fig. 13. Both membranes are considered hydrophilic because the values are below 90˚, which is the upper limit for hydrophilic membrane. MA (53.39˚) was found to be more hydrophilic than MB (62.46˚). The surface charge and hydrophobicity of the membrane surface interact

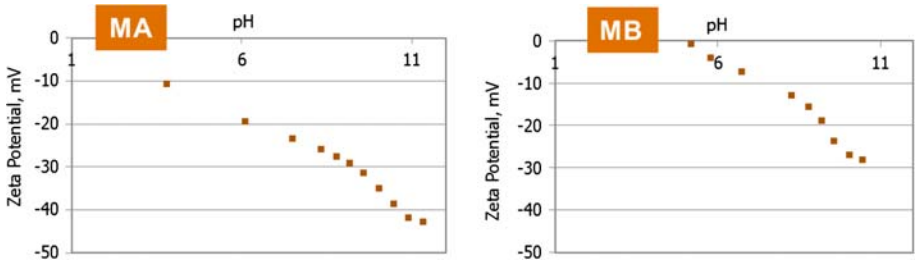

Fig. 12. Zeta potential of SDI membranes using 10 mM NaCl electrolyte solution.

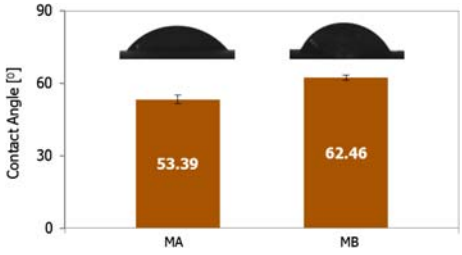

Fig. 13. Contact angles of SDI membranes, MA and MB.

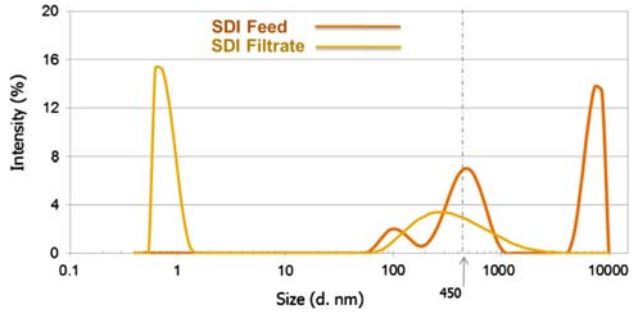

Fig. 14. Particle size distribution of SDI feed and filtrate of P1.

with the same properties mentioned for foulant resulting membrane–foulant absorptive interaction, which clearly influences the SDI. However, compared to dead end hydrodynamic mode of the filtration and size exclusion mechanisms of membrane, the absorptive interaction might not be the determining factor influencing the SDI value.

3.3. Particle removal during SDI filtration

SDI is specifically developed to assess the potential of particulate fouling of RO feedwater. Thus, particulate removal analysis is a suitable tool to understand the role of particulate deposit to the membrane quantification. Particle removal study was conducted to SDI feedwater and SDI filtrates.

Particulate removal study for SDI measurement of the seawater (P1) is shown in Fig. 14. Several peaks can be observed at the SDI feedwater particle distribution curve: a peak around 100 nm, another peak at 450 nm, which is the nominal membrane pore size, and a peak, which belongs to the big particle size fraction. Subsequent to SDI measurement, which is represented by SDI filtrate, big particle fraction was completely removed. Another two peaks replaced by a peak lay in the middle of previous two peaks, indicates partial removal of particle with particular corresponding size. A appearance of peak in the range of small size proves the particle removal during SDI measurements shifting the size distribution curve towards small size direction. Aforementioned particle removal is corresponding to SDI_5 value of 16.03%/min.

Particulate removal study for SDI measurement of RO feedwater (P3) is shown in Fig. 15. The same trend showed in the study of P1 was also observed in P3. A peak at big particle size was completely removed from SDI filtrate. The two peaks surrounding nominal pore size of SDI membrane were partially removed and became a single peak. Aforementioned particle removal corresponds to SDI_{15} value of 3.2%/min and turbidity of 0.12. Sequential SDI filtrations were conducted. These experiments utilized the filtrate from subsequent SDI filtration, which is then tested for its SDI value. The final step of sequential filtration is sec-

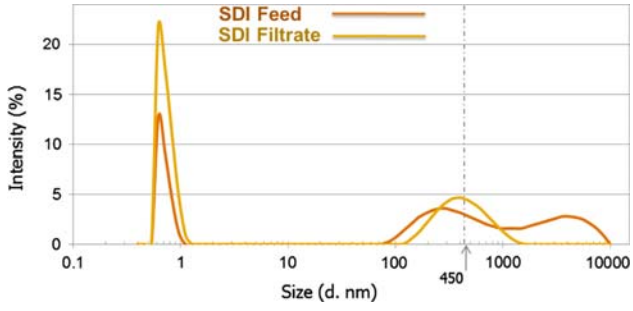

Fig. 15. Particle size distribution of SDI feed and filtrate of P3.

ond filtration that is limited by water sample required to perform the experiments.

Interesting results from sequential SDI filtration were found. Reduction of SDI value occurred in original feedwater, first filtrate, and finally second filtrate with specific values of 3.2, 2.2, and 1.9, respectively (Table 1). Given the knowledge from the particle removal study, the presence of SDI values from the measurement of the filtrate implied that the small particles below the nominal pore size of membrane were responsible for the quantification of SDI. However, turbidity analyses of the filtrate (<0.05) showed evidence of the insignificant amount of particle present in the filtrates. This fact indicates nonparticle-related foulant represented by the values of SDI. Further investigation of the latter hypothesis is presented in the next section. On the other hand, the modified fouling index (MFI) values obtained from the slope of linear curves of t/V vs. accumulated filtrate volume (V) using the classical cake filtration model (Eq. (4)) [11], are more predictive despite MFI has no standard values for practical comparison.

$$\frac{t}{V} = \frac{\mu \times R_M}{\Delta P \times A_M} + \frac{\mu \times I}{2 \times \Delta P \times A_M^2} \times V \quad (4)$$

where t is the time, μ is the water viscosity, A_M is the membrane area, and I is the fouling potential index.

3.4. Influence of particles concentration and size

Polystyrene microparticles with different average particle size and concentration were used to simulate the particulate foulant in the water. Experiments with different concentrations aimed for the trend of SDI values with different amounts of particulate foulants. In addition, study of particle size intended to give the critical size of particles than significantly influenced the quantification of SDI. Furthermore, this information will support the assumption of fouling mechanism that occurs in SDI filtration. Figs. 16 and 17 give the results of the influence of particle concentration and size.

Table 1
Sequential SDI determination

Feed water	Turbidity (NTU)	SDI (%/min)	MFI (s/L^2)
Seawater (P1)	1	16.04	283.73
Pretreated seawater (P3)	0.12	3.2	5.22
First SDI filtrate	0.05	2.2	1.03
Second SDI filtrate	0.05	1.9	≪
Permeate of 10 kDa membrane	0.05	1.4	≪

As observed in Fig. 14, SDI values increased with the increase in particle concentration for all range of particle sizes, implying more particles available to foul the membrane as the concentration increases. However, the factors of increment to the SDI values were different for each particle size. Substantial increases were observed for 0.1 μm particles with the concentration and the increments reduced in the sequence of 1 μm, mixed sizes, and 0.5 μm.

The difference of sensitivity given by the size of particles to SDI quantification might be related by the mechanism of the specific particle size to foul the membrane. Certain amount of particles that significantly block the filter pores formed a cake layer as a matter of fouling, increasing the concentration caused by insignificant difference as shown by the trend of 0.5 μm particle. On the contrary, if the amount of particles is not sufficient to bring about significant membrane fouling, the increasing amount of particles will be affected because more particles were present and ready to foul the membrane as shown by the trend of 0.1 and 1 μm.

The study of particle size on SDI is shown in Fig. 17. At a certain concentration, the 0.1 μm particles resulted in the lowest value of SDI, and then increased for 1 μm, mixed sizes, and 0.5 μm, consecutively. This trend was observed for all variations of concentration. In relation of 0.45 μm as the nominal pore size of SDI membrane, the 0.1 μm particles as expected, mainly passed through the filter during filtration and left an insignificant quantification of SDI. Some particles may foul the membrane internally and expressed by an SDI value. This fact also proves that small particles are also responsible for the SDI quantification.

In the case of 0.5 and 1 μm particles, both fractions foul the membrane by cake formation with a slight possibility of internal and partial clogging of the filter based on the nominal membrane pore size and the PSD. The influence of 0.5 μm observed to be more severe than 1 μm particle. The character of possible cake formation can explain these phenomena on the membrane surface. Comparing both sizes, 0.5 μm particles have more possibilities to penetrate inside the pores (size around 0.45 μm) of membranes and block those pores compared to large size particle (1 μm). Furthermore, cake with 0.5 μm particles will form in a more compact way, with small vacant space between particles within the cake structure. In other words, the porosity of 0.5 μm particle cake was lower and provided more resistance for water to flow com-

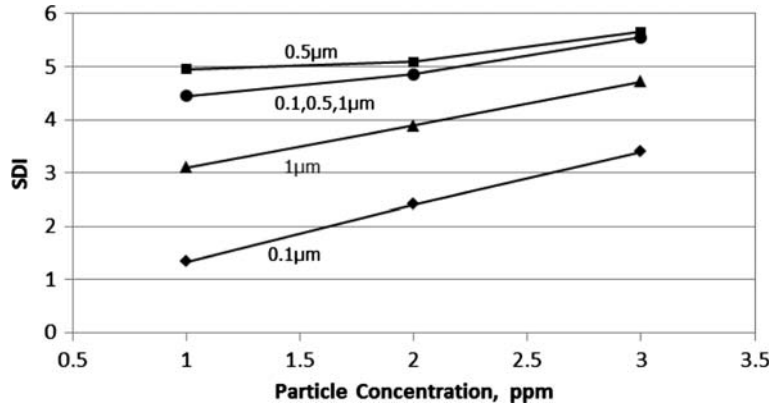

Fig. 16. The influence of particle concentration on SDI.

pared to 1 µm particle cake. In the case of the mixture of three sizes used in SDI measurement, the values were found to be nearer to 0.5 µm SDI values. Thus, it is clear that the 0.5 µm particles play a significant role in the SDI quantification as they are dominating the partial and internal fouling before cake formation. This case can be generalized to the size that is comparable or close to the nominal pore size of the membrane that is expected to be substantially expressed in SDI measurements. Also, organic matter adsorption might contribute to SDI quantification [27]. Our earlier SDI results shown in Figs. 14 and 15 were also confirming our conclusion that with increase of 0.5 µm particles (where particle average size is equivalent to nominal pore size of the membranes), SDI values reasonably increased.

The studied particle concentration and size parameters demonstrated that at the same particle concentration, the measured SDI values varied based on the particle size used. The optimal values correspond to the water containing particles with size close to the SDI membrane pore size (0.5 µm and mixed sizes). Again, this result showed the SDI limitation of fouling prediction of small particles or colloids, which can cause a severe fouling, while representing low SDI values. Formation of the cake on SDI membrane will also affect the sensitivity of the measurement by forming secondary filter with lower porosity and permeability than SDI membrane itself. Furthermore, the filtration mechanism becomes more complex to comprehend when partial fouling occurs ahead of cake filtration, which is the most probable case with feedwater containing small particles.

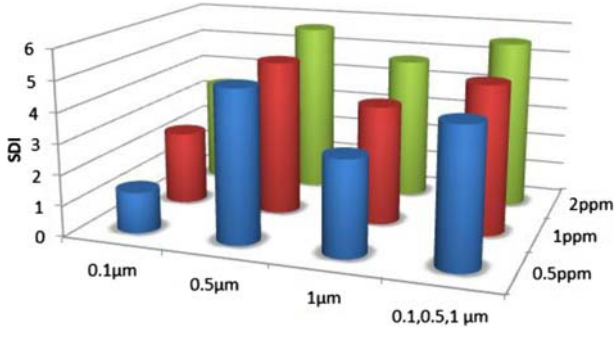

Fig. 17. The influence of particle size on SDI.

4. Alternative fouling indices

The failure of SDI accurately predicts the fouling potential attracted several researchers to develop new fouling indices. Hong et al. [28] utilized flow field-flow fraction (Fl-FFF) to overcome the problem. The resulted Fl-FFF analyses demonstrated that estimation of fouling tendency of feedwater with the different foulants and salinity level was possible to perform both qualitatively and quantitatively.

Alteration of filter pore size of MFI to be 0.05 µm was done after practical observation to the existing MFI that does not correlate the colloidal fouling and concludes that particles below 0.45 µm is probable cause to the problem [29]. Development of fouling indices based on pore size aiming smaller particle to be captured by utilizing smaller pore size membranes yielded MFI-UF that uses UF membrane [30] and MFI-NF in which NF is used [31]. Yu et al. [32] developed a new approach to evaluate the fouling potential in RO systems. A multiple membrane array system using a series of membranes with different pore sizes was used. MFI was measured during each separation representing particles, colloidal, and organic removal through MF (0.45 µm), UF (100 kDa), and NF (10 kDa) membranes, respectively.

Combine fouling index (CFI) was also proposed by Choi et al. [33] to include the contribution of particles, hydrophobic matters, colloids, and organics to RO/NF fouling. CFI is weighed factors combining three kinds of MFI: MFI-HL which relates to the usage of hydrophilic MF membrane, MFI-HP which corresponds to hydrophobic MF membrane, and MFI-UF that considers hydrophilic UF membrane.

In terms of the filtration system, existing MFI-UF at constant pressure mode of filtration was improved by MFI-UF at constant flux. The problem was the flux in constant pressure was significantly higher and does not represent the actual RO system. The MFI-UF constant flux was anticipated to nearly mimic fouling at the membrane surface, enhance fouling prediction accuracy, and imitate actual RO operation [34,35].

Development of MFI in regard to the hydraulic system of filtration came up with crossflow sampler (CFS)-MFI to replace dead end filtration MFI. This method considers flux and crossflow velocity that mimics the character of RO filtration [36]. Comparison and investigation of MFI-UF constant pressure, constant flux, CFS-MFI has been studied along with coupled effect which resulted from cake-enhanced osmotic pressure and colloidal fouling in RO using CFS [37,38].

Unfortunately, the protocols to perform aforementioned developed fouling indices, which are more accurate and informative in terms of fouling prediction, can be considered as impractical and complicated to be used by RO plants operators as routine basis compared to SDI.

5. Conclusions

Assessment of SDI as fouling propensity parameter in RO desalination has been studied in this work, aiming to the evaluation of its reliability. Variation of SDI values was obtained using two different commercial membranes in the same operating conditions. In addition, this inconsistency was confirmed when comparing *in-situ* (KAUST–SWRO Plant) and laboratory measurements. These findings indicated the low level of precision and accuracy of the SDI test. The experimental apparatus and operational practices contributed to the inconsistent values of SDI. Thus, the result of SDI may be over/underestimating the fouling tendency, which clearly jeopardizes the prediction of fouling in RO operation.

It has been noticed that particle size and concentration played a significant role in SDI quantification. Fraction of small particles (below 0.45 μm) and particles with size close to membrane pore size are being represented more in SDI values. However, the particles are not the sole factor that being quantified in SDI as showed by turbidity assisted SDI measurements. The emerging reason is nonfouling factors, such as hydrodynamic alteration during measurements, as shown in the study of SDI for clean water. Also, natural organic matter adsorption might be contributed to SDI quantification. These nonfouling-related factors will mislead the judgment of fouling tendency.

In order to overcome the reliability problem in fouling indices, development should be done in either improvement to the existing index or applying a new method of fouling estimation. The aim is to reduce the fouling occurrence in RO operation by accurately predicting the fouling propensity of feedwater, better judgment of pretreatment performance, and ability to model fouling rate of RO.

References

[1] N. Ghaffour, The challenge of capacity-building strategies and perspectives for desalination for sustainable water use in MENA, Desalin. Water Treat. 5 (2009) 48–53.
[2] N.R.G. Walton, Some observations on the considerable variability of silt density index results due to equipment, filter and operator variables, Desalination 61 (1987) 201–210.
[3] A. Nahrstedt, J. Camargo-Schmale, New insights into silt density index and modified fouling index measurements, Water Science & Technology: Water Supply – WSTWS 8(4) (2008) 401–411.
[4] A. Alhadidi, Limitations, Improvements, Alternatives for the Silt Density Index, Thesis, Enschede, 2011. Available from: <http://www.doc.utwente.nl/76066/>.
[5] A. Mosset, V. Bonnely, M. Petry, M.A. Sanz, The sensitivity of SDI analysis: From RO feed water to raw water, Desalination 222 (2008) 17–23.
[6] K. Burashid, A.R. Hussain, Seawater RO plant operation and maintenance experience: Addur desalination plant operation assessment, Desalination 165 (2004) 11–22.
[7] C.D. Moody et al., Yuma desalting test facility: Foulant component study, Desalination 47 (1983) 239–253.
[8] W. Arras, N. Ghaffour, A. Hamou, Performance evaluation of BWRO desalination plant – a case study, Desalination 235 (2009) 170–178.
[9] N. Ghaffour, Modelling of fouling phenomena in cross-flow ultrafiltration of suspensions containing suspended solids and oil droplets, Desalination 167 (2004) 281–291.
[10] A. Alhadidi, B. Blankert, A.J.B. Kemperman, J.C. Schippers, M. Wessling, W.G.J. van der Meer, Effect of testing conditions and filtration mechanisms on SDI, J. Membr. Sci. 381 (2011) 142–151.
[11] J.C. Schippers, J. Verdouw, The modified fouling index, a method of determining the fouling characteristics of water, Desalination 32 (1980) 137–148.
[12] N. Ghaffour, M.W. Naceur, N. Drouiche, H. Mahmoudi, Use of ultrafiltration membranes in the treatment of refinery wastewaters, Desalin. Water Treat. 5 (2009) 159–166.
[13] S.G. Yiantsiosand, A.J. Karabelas, An assessment of the silt density index based on RO membrane colloidal fouling experiments with iron oxide particles, Desalination 151 (2003) 229–238.
[14] S.S. Kremen, M. Tanner, Silt density indices (SDI), percent plugging factor (%PF): Their relation to actual foulant deposition, Desalination 119 (1998) 259–262.

[15] M. Ando, S. Ishihara, H. Iwahori, N. Tada, Peculiar or unexpected behavior of silt density index of pretreated seawater for RO, Desalination, Proceeding of IDA World Congress, Bahamas, BAH03-071, 2003.
[16] A. Brehant, V. Bonnelye, M. Perez, Comparison of MF/UF pretreatment with conventional filtration prior to RO membranes for surface seawater desalination, Desalination 144 (2002) 353–360.
[17] C.K. Teng, M.N.A. Hawlader, A. Malek, An experiment with different pretreatment methods, Desalination 156 (2003) 51–58.
[18] J.D. Zhang, Y.W. Liu, S.M. Gao, C.Z. Li, F. Zhang, H.M. Zen, C.S. Ye, Pilot testing of outside-in UF pretreatment prior to RO for high turbidity seawater desalination, Desalination 189 (2006) 269–277.
[19] P.H. Wolf, S. Siverns, S. Monti, UF membranes for RO desalination pretreatment, Desalination 182 (2005) 293–300.
[20] D.F. Halpern, J. McArdle, B. Antrim, UF pretreatment for SWRO: Pilot studies, Desalination 182 (2005) 323–332.
[21] Dow FILMTEC SW Seawater Reverse Osmosis Element, 2011. Available from: <http://www.dowwaterandprocess.com/products/ronf.htm>.
[22] Hydranautics, ESPA, LFC, CPA ESNA and SWC RO Seawater Element, 2011. Available from: <http://www.membranes.com/pdf/HYDRABrochure.pdf>.
[23] Koch RO Spiral Elements. Available from: <http://www.kochmembrane.com/support_ro_lit.html>.
[24] Toray, RO Elements Catalog, 2011. Available from: <http://www.toraywater.com/catalog/catalogbase.aspx?mode=catalog>.
[25] Toyobo, HR, HM, HB, and HL Series Seawater Desalination, 2011. Available from: http://www.toyobo.co.jp/e/seihin/ro/index.htm.
[26] C.J.M.v. Rijn, Chapter 7: Microfiltration in Membrane Science and Technology, Elsevier, 10 (2004) 169–253.
[27] A. Ramdani, S. Taleb, A. Benghalem, N. Ghaffour, Removal of excess fluoride ions from Saharan brackish water by adsorption on natural materials, Desalination 250 (2010) 408–413.
[28] K. Hong, S. Lee, S. Choi, Y. Yu, S. Hong, J. Moon, J. Sohn, J. Yang, Assessment of various membrane fouling indexes under seawater conditions, Desalination 247 (2009) 247–259.
[29] S.F.E. Boerlage, M.D. Kennedy, P.A.C. Bonne, G. Galjaard, J. C. Schippers, Prediction of flux decline in membrane systems due to particulate fouling, Desalination 113 (1997) 231–233.
[30] S.F.E. Boerlage, M.D. Kennedy, I. Bremere, G.J. Witkamp, J.P. Van Der Hoek, J.C. Schippers, The modified fouling index using ultrafiltration membranes (MFI-UF): Characterisation, filtration mechanisms and proposed reference membrane, J. Membr. Sci. 197 (2002) 1–21.
[31] S. Khirani, R. Ben Aim, M.-H. Manero, Improving the measurement of the modified fouling index using nanofiltration membranes (NF-MFI), Desalination 191 (2006) 1–7.
[32] Y. Yu, S. Lee, K. Hong, S. Hong, Evaluation of membrane fouling potential by multiple membrane array system (MMAS): Measurements and applications, J. Membr. Sci. 362 (2010) 279–288.
[33] J.-S. Choi, T.-M. Hwang, S. Hong, A systematic approach to determine the fouling index for a RO/NF membrane process, Desalination 238 (2009) 117–127.
[34] S.F.E. Boerlage, M. Kennedy, Z. Tarawneh, R. De Faber, J.C. Schippers, Development of the MFI-UF in constant flux filtration, Desalination 161 (2004) 103–113.
[35] S. Salinas, N. Ghaffour, M. Kennedy, J. Schippers, G. Amy, New concepts in fouling indices, AWWA/AMTA Membrane Technology Conference, February 27—March 1, 2012, Phoenix, USA.
[36] L.N. Sim, Y. Ye, V. Chen, A.G. Fane, Crossflow sampler modified fouling index ultrafiltration (CFS-MFIUF)–An alternative Fouling Index, J. Membr. Sci. 360 (2010) 174–184.
[37] M.A. Javeed, K. Chinu, H.K. Shon, S. Vigneswaran, Effect of pre-treatment on fouling propensity of feed as depicted by the modified fouling index (MFI) and cross-flow sampler-modified fouling index (CFS-MFI), Desalination 238 (2009) 98–108.
[38] L.N. Sim, Y. Ye, V. Chen, A.G. Fane, Comparison of MFI-UF constant pressure, MFI-UF constant flux and crossflow sampler-modified fouling index ultrafiltration (CFS-MFIUF), Water Res. 45 (2011) 1639–1650.